MSAS – Assignment #2: Modeling

Fernando Aranda Romero, 213686

Exercise 1

The rocket engine in Figure 1 is fired in laboratory conditions. With reference to Figure 1, the nozzle is made up of an inner lining (k_1), an inner layer having specific heat c_2 and high conductivity k_2, an insulating layer having specific heat c_4 and low conductivity k_4, and an outer coating (k_5). The interface between the conductor and the insulator layers has thermal conductivity k_3.

1.1) Part 1: Parameters definition

Select the materials of which the nozzle is made of*, and therefore determine the values of k_i ($i = 1, \dots, 5$), c_2, and c_4. Assign also the values of ℓ_i (i=1,...,5), L, and A in Figure 1.

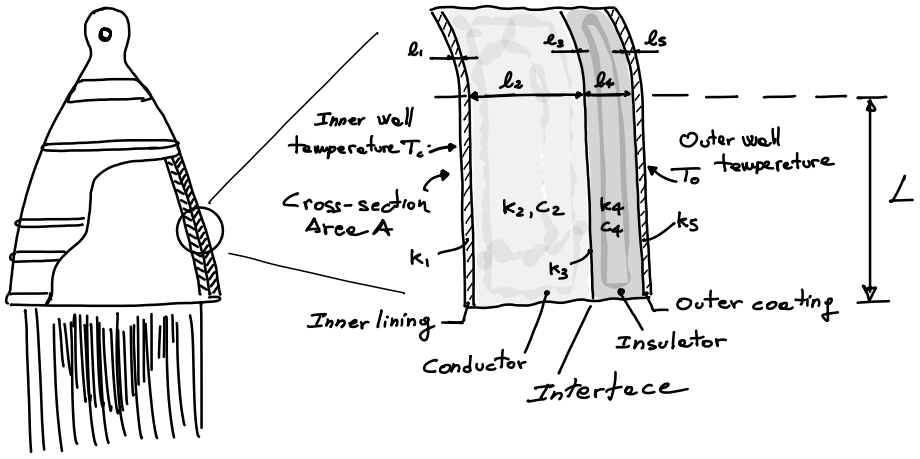

Figure 1: Real thermal system.

1.2) Part 2: Causal modeling

Derive a physical model and the associated mathematical model using one node per each of the five layers and considering that only the conductor and insulator layers have thermal capacitance. The inner wall temperature, T_i, as well as the outer wall temperature, T_o, are assigned. Using the mathematical model, carry out a dynamic simulation in MATLAB to show the temperature profiles across the different sections. At initial time, $T_i(t_0) = T_o(t) = 20$ C°. When the rocket is fired, $T_i(t) = 1000$ C°, $t \in [t_1, t_f]$, following a ramp profile in $[t_0, t_1]$. Integrate the system using $t_1 = 1$ s and $t_f = 60$ s.

1.3) Part 3: Acausal modeling

a) Reproduce in Simscape the physical model derived in Part 2. Run the simulation from $t_0 = 0$ s to $t_f = 60$ s and show the temperature profiles across the different sections. Compare the results with the ones obtained in point 1.2). b) Which solver would you choose? Justify

*The interface layer is not made of a physically existing material, though it produces a thermal resistance. For this layer, the value of the thermal resistance R_3 can be direcly assumed, so avoiding to choose k_3 and ℓ_3.

the selection based on the knowledge acquired from the first part of the course. c) Repeat the simulation in Simscape implementing two nodes for the conductor and insulator layers and show the temperature profiles across the different sections.

(15 points)

Doing a brief literature review, the selected parameters to characterise the rocket nozzle are introduced in Table 1. In the case of the interface node, a convention coefficient of $h_c = 1500$ W/m2K is chosen to model its resistance.

Node	Material	k [W/m K]	c_p [J/kgK]	l [mm]	ρ [kg/m^3]	T_{melt} [°C]
1	Graphite	24	–	5	–	3650
2	Molybdenum TZM	118	250	40	10160	2620
4	Silica	1.4	700	10	2200	1713
5	A286	17.8	–	5	–	1370

Table 1: Rocket nozzle parameters

To develop the physical and mathematical models of the problem the following assumptions are made:

1. The temperature nodes are located in the middle of each the layer
2. The heat flux at the nodes without thermal capacitance is assumed to instantaneously achieve the steady state condition with the conductor and insulator variations
3. The variations in the heat flux are caused by the nodes with thermal capacitance

Under these assumptions and applying the electrical similarity, the physical model shown in Figure 2 is retrieved.

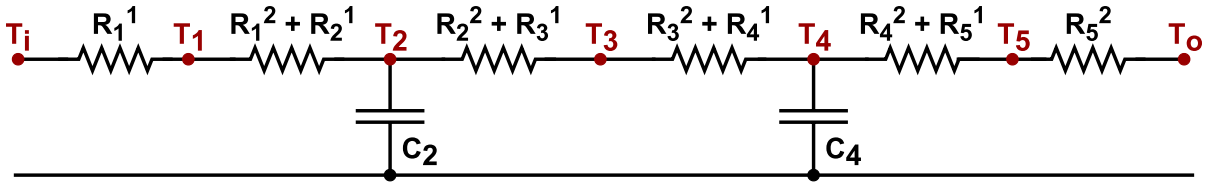

Figure 2: Exercise 1 physical model

However, due to Assumption 3, the previous model can be condensed into the one displayed in Figure 3. In this way, the numerical integration is only applied to the conductor and insulator layers, and the results are used to retrieve the temperature in the remaining nodes.

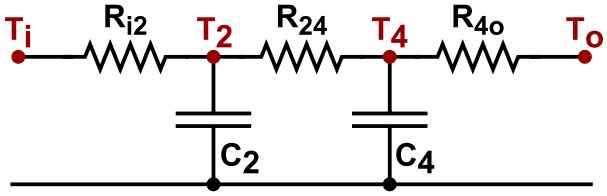

Figure 3: Exercise 1 condensed physical model

After presenting the physical model, the mathematical model can be derived. The first step of this process is to estimate the resistance and capacitance values for each node. To do so, Equation 1 is applied, where the area A is assumed to be 1 m^2 to ease the results understanding.

$$\begin{cases} R_j = \dfrac{l_j}{k_j\, A} & \text{for } j = 1,\ 2,\ 4,\ 5 \\ R_3 = \dfrac{1}{h_c\, A} & \\ C_j = A\, \rho_j\, l_j\, c_{p-j} & \text{for } j = 2,\ 4 \end{cases} \tag{1}$$

The resistances of each node can be then used to compute the resistance appearing in the physical model of Figure 3 using Equation 2

$$\begin{cases} R_{i2} = R_1 + \dfrac{R_2}{2} \\ R_{24} = \dfrac{R_2}{2} + R_3 + \dfrac{R_4}{2} \\ R_{4o} = \dfrac{R_4}{2} + R_5 \end{cases} \tag{2}$$

By applying these resistances and the capacitance values, the differential equations describing the temperature evolution of the conductor and insulator nodes are derived by computing the heat fluxes between the nodes appearing in Figure 3. The system to be integrated is described in Equation 3. Even though it is not requested, the *Matlab* function implementing this system includes the whole period from $t_0 = 0$ s to $t_f = 60$ s. In this way, the comparison between the causal and acausal results is more significant.

$$\begin{cases} \dot{T}_2 = \dfrac{R_{24}\, T_i - (R_{i2} + R_{24})\, T_2 + R_{i2}\, T_4}{R_{i2}\, R_{24}\, C_2} \\ \dot{T}_4 = \dfrac{R_{4o}\, T_2 - (R_{24} + R_{4o})\, T_4 + R_{24}\, T_o}{R_{24}\, R_{4o}\, C_4} \end{cases} \tag{3}$$

Finally, once these two equations are integrated, Equation 4 retrieves the temperatures at nodes 1, 3 and 5 for each integration step by applying Assumption 3.

$$\begin{cases} T_1 = T_i - \dfrac{R_1\, (T_i - T_2)}{2\, R_{i2}} \\ T_3 = T_2 - \dfrac{(R_2 + R_3)\, (T_2 - T_4)}{2\, R_{24}} \\ T_4 = T_o + \dfrac{R_4\, (T_4 - T_o)}{2\, R_{4o}} \end{cases} \tag{4}$$

For the solver selection, a study of the differential system eigenvalues is performed. To do so, the Jacobian of the system shown in Equation 3 is retrieved and introduced in Equation 5. Then, the eigenvalues of this matrix are obtained and displayed in Figure 4.

$$\frac{\partial \dot{\underline{T}}}{\partial \underline{T}} = \begin{bmatrix} \dfrac{-(R_{i2} + R_{24})}{C_2\, R_{i2}\, R_{24}} & \dfrac{1}{C_2\, R_{24}} \\ \dfrac{1}{C_4\, R_{24}} & \dfrac{-(R_{24} + R_{4o})}{C_4\, R_{24}\, R_{4o}} \end{bmatrix} \tag{5}$$

The differential problem derived from the rocket nozzle properties introduced in Table 1 is non-stiff, therefore, *ode45* is the solver selected to integrate both the causal and acausal simulations so the comparison of the results can be more meaningful. A value of $1e-11$ is used for the relative and absolute integration tolerances and, to have the same number of integration steps, the time vector retrieved from *Simscape* is used for the causal integration.

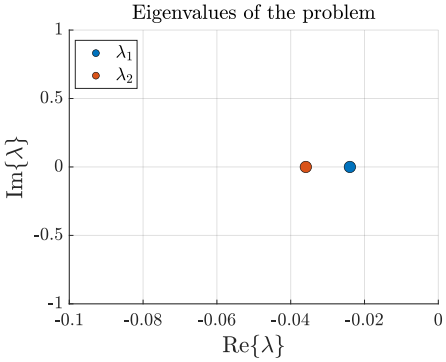

Figure 4: Eigenvalues of the causal problem

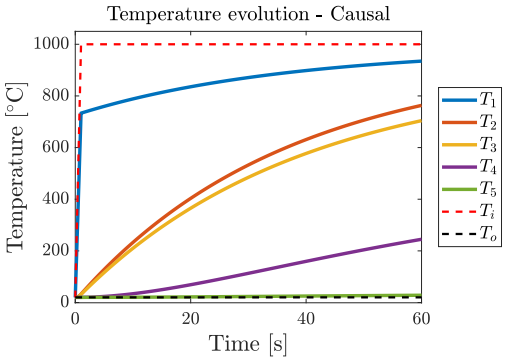

Figure 5: Temperature evolution - Causal approach

Figure 5 shows that all the layers are under the melting point temperature, meaning that the selected nozzle properties are appropriate for this application.

Figures 6 and 7 show the results of the *Simscape* simulation and its comparison with the causal solution. The differences between both approaches are negligible as they are in the order of 10^{-8} meaning that both approaches have been properly implemented.

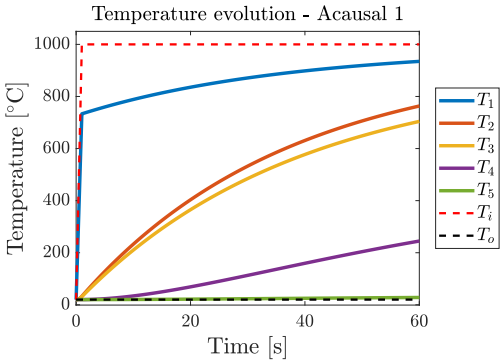

Figure 6: Temperature evolution - 1 node acausal approach

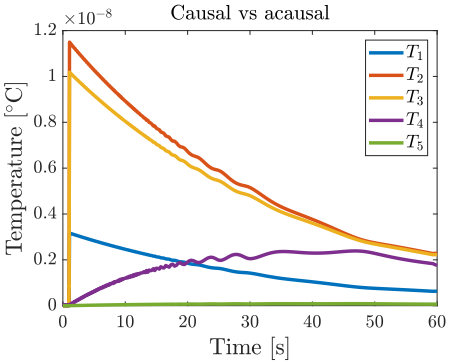

Figure 7: Comparison between causal and acausal results

Finally, a *Simscape* model including two nodes for the conductor and insulator layers is developed. Figure 8 displays the temperature profiles in each layer, also in this case all the temperatures are under the melting points, as expected. To have a better understanding of how this change affects the results, Figure 9 is used to compare both acausal solutions, 1 and 2 nodes. The temperature difference in all the layers is remarkable, meaning that the 1-node implementation can be widely improved by implementing more nodes in the layers. Therefore, to have more accurate results, the number of nodes per layer should be increased.

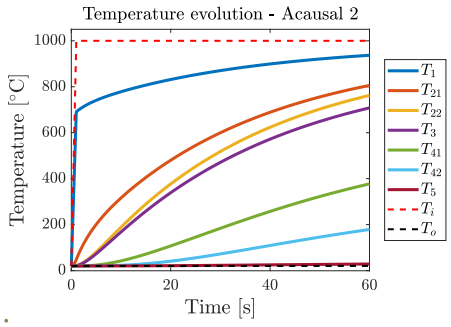

Figure 8: Temperature evolution - 2 node acausal approach

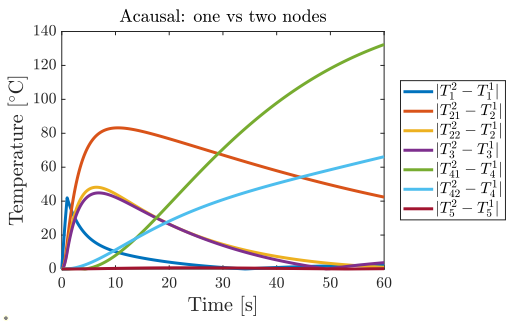

Figure 9: Comparison between 1 and 2 nodes acausal results

Exercise 2

The real system of an electric propeller engine is depicted in Figure 10. It is composed by a DC permanent magnet motor which drives a propeller shaft. Between the motor and propeller shaft there is a single stage gear box to regulate the angular speed ratio. Moreover, to avoid overheating of the gear unit, the system is augmented by a cooling system where a fluid exchanges heat with the gear box itself. In Figure 11 a functional breakdown structure of the system is shown.

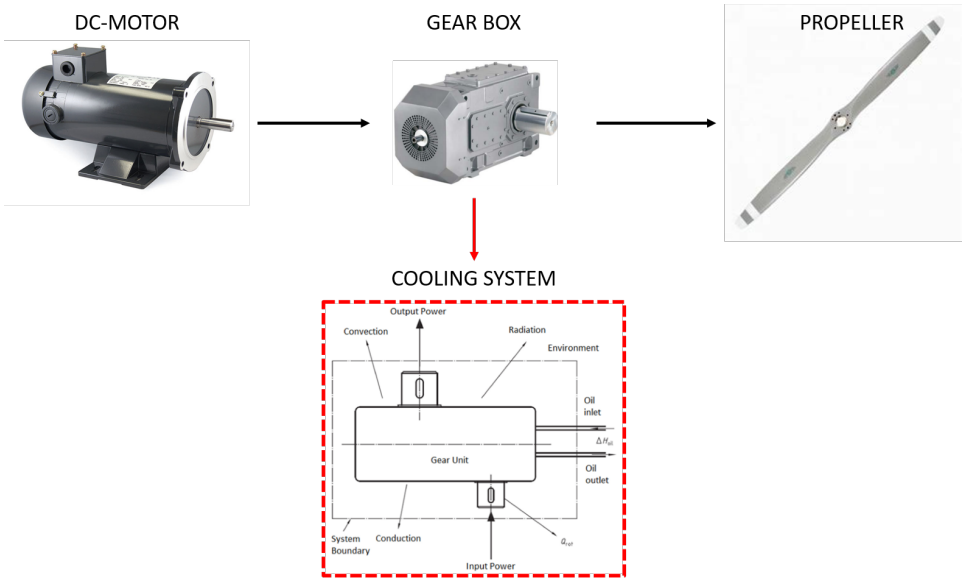

Figure 10: Real system.

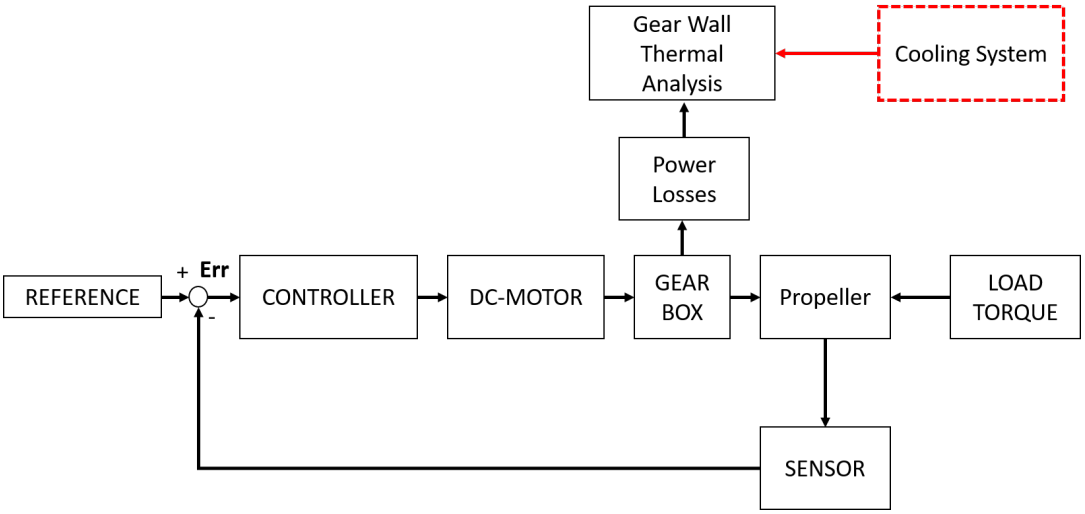

Figure 11: Functional block scheme of the system.

2.1) Part 1: Propeller Electric Engine

Considering the real system in 10 **without** the cooling part, you are asked to:

1. Extract a physical model highlighting assumptions and simplifications.
2. Reproduce the model in acausal manner in Dymola.

3. According to the block scheme in 11, tune a controller (e.g., a PID controller) such that the motor input voltage remains less than 200 V and the error signal **Err** is less than 0.1 rad/s after 10 s.

4. Study the Gear box temperature and heat flux for a simulation time of $\mathbf{t_f} = 120$ s (considering only conduction as heat transfer).

5. Discuss the simulation results and the integration scheme used

For the simulation part, you shall consider: the DC motor data listed in Table 2; the gear box data listed in Table 3, with loss parameters in Table 4; a propeller made of **aluminium** with nominal angular speed $\hat{\omega}$ and a nominal quadratic speed load torque $\hat{T}_{load}$ acting on it (Table 5). The reference angular speed signal to be tracked by the propeller is given in Figure 12.

Table 2: DC motor data

Parameter	Value	Unit
Coil Resistance	0.1	Ω
Inductance	0.01	H
Motor Inertia	0.001	kg m^2
Motor Constant	0.3	Nm/A

Table 3: Gear Box data

Parameter	Value	Unit
Mass	3	kg
Gear ratio	2	[-]
Specific heat	1000	J/(kg K)
Thermal Conductivity	100	Wm/K

Table 4: Gear Box Loss Table

Driver angular speed [rad/s]	Mesh efficiency[-]	Bearing friction torque [Nm]
0	0.99	0
50	0.98	0.5
100	0.97	1
210	0.96	1.5

Table 5: Propeller data

Parameter	Value	Unit
Diameter	0.8	m
Thickness	0.01	m
$\hat{\omega}$	210	rad/s
$\hat{T}_{load}$	100	Nm

2.2) Part 2: Cooling System

After the previous gear unit thermal analysis, now consider the steady-state condition reached by the propeller engine at the end of the simulation to model and simulate a single **fixed** volume flow rate cooling system (as shown in Figure 10) for the gear unit and considering only **convection** as heat transfer. In particular, you are asked to:

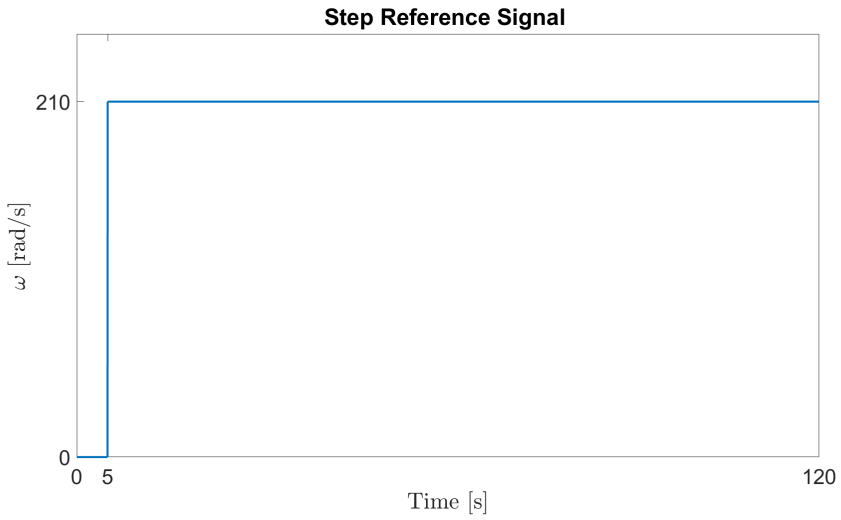

Figure 12: Angular speed reference for the propeller.

1. Derive a physical model highlighting assumptions and simplifications.
2. Reproduce the acausal model in Dymola.
3. Tune the cooling system in terms of volume flow rate, control logics, and initial fluid storage temperature such that:
   (a) the gear unit is kept between 40°C and 60°C.
   (b) the source tank does not get empty before the end simulation time
   (c) the storage tanks have a maximum height of 0.8 m and cross section area of 0.01 m^2
   (d) the system shall have a recirculating capability in order to exploit the outlet fluid for a next cooling process (when the source tank get empty)
   (e) the sink heated fluid is kept between 5°C and 10°C.
   (f) the power consumption of the thermal system shall be no more than 6 kW
4. Discuss the simulation results and the integration scheme used

For the simulation part consider properties of water at 10°C as cooling incompressible fluid (convective thermal conductance $\lambda_{conv} = 300$ W/K) and the cylindrical pipe line data listed in Table 6. The simulation shall last at least $\mathbf{t_{sim}} = 300$ s starting with no water along the pipe.

Table 6: Pipe line properties

Parameter	Value	Unit
Diameter	4	cm
Length	40	cm
Geodetic height	0	m
Friction losses	0	[-]

(15 points)

2.1) Part 1: Propeller Electric Engine

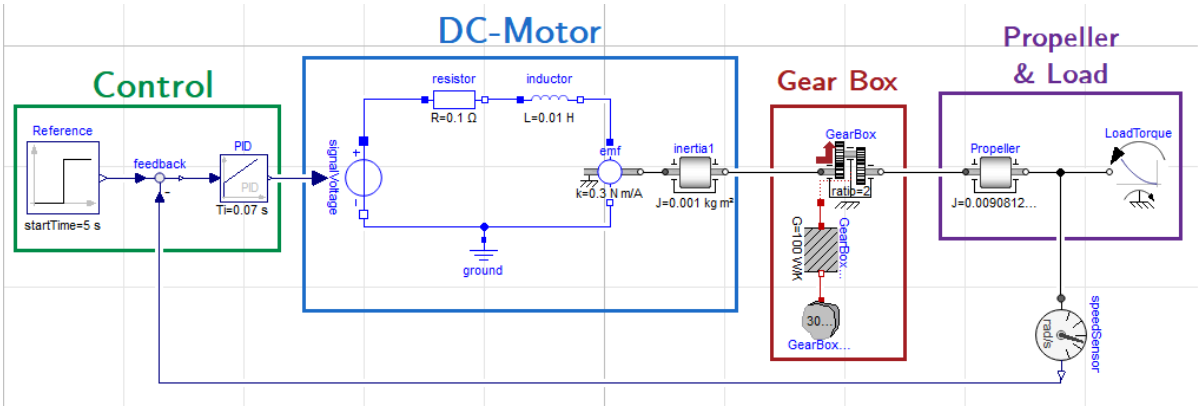

Figure 13: Propeller electric engine physical model

The physical model shown in Figure 13 is retrieved by applying the following assumptions and simplifications:

1. The DC-Motor is modelled as the combination of resistance, inductor, electric/mechanic transformer (emf) and inertia. This allows a significant reduction in the number of equations
2. The gear box is assumed to be a lossy gear whose power losses heat the gear box wall through conduction
3. The gear box wall is a simple heat capacitor that stores heat
4. The propeller is modelled as a simple 1-D rotational inertia and the load torque is a quadratic speed-dependent torque
5. The propeller is assumed to be a cylindrical rod spinning around its centre
6. The control logic is performed by a PID, whose output is the input of a signal voltage element to control the DC-Motor

To prepare the *Dymola* model for the simulation, the PID parameters and the propeller equivalent inertia need to be obtained. Regarding the propeller inertia, it can be retrieved by applying Assumption 5 and the system defined in Equation 6, where t_{prop} is the propeller thickness, D_{prop} the propeller diameter and $\rho_{prop} = 2710$ kg/m^3 the aluminium density. On the other hand, Table 7 retrieves the PID parameters used for the simulation.

$$\begin{cases} V_{prop} = \dfrac{\pi\, t_{prop}^2\, D_{prop}}{4}\ [\mathrm{m}^3] \\ M_{prop} = \rho_{prop}\, V_{prop}\ [\mathrm{kg}] \\ J_{prop} = \dfrac{M_{prop}\, D_{prop}^2}{12}\ [\mathrm{kgm}^2] \end{cases} \tag{6}$$

Gain [-]	**Integration Constant** [s]	**Derivative Constant** [s]
1.2	0.07	0.02

Table 7: PID parameters

Before performing the simulation, it is necessary to understand the appropriate solver to be used. The physical model introduced in Figure 13 is composed of mechanical and electrical components. It is well known that these two domains have very different response times and temporal behaviours. For instance, the electric domain has a very fast time response. Because of this, Figure 13 probably models a stiff system. Given this qualitative analysis, the best solver selection would be an A-stable or implicit integrator scheme. The default *Dymola* solver, *DASSL* is then selected as it is an implicit, higher-order, multi-step solver with a step-size control which allows the integration of domains with very different temporal behaviours. Now the simulation can be run and the results can be extracted.

Figure 14 shows the error of the propeller angular speed with respect to the reference provided in Figure 12 which meets the requirement specified in the exercise statement. Figure 15, instead, displays the input voltage of the DC-Motor electro-mechanic transformer, which is always under the specified 200 V threshold.

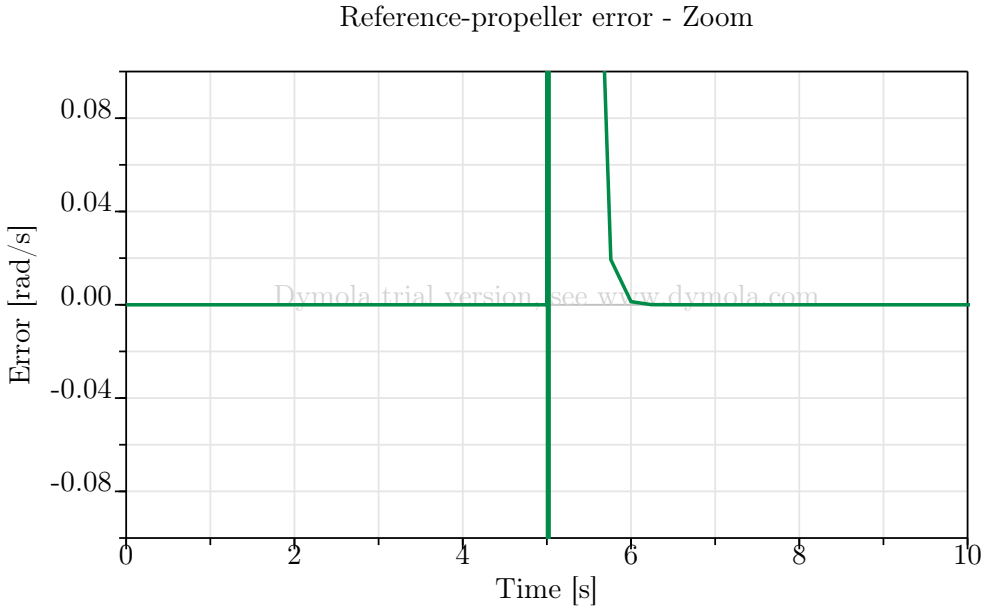

Figure 14: Reference-propeller angular speed error evolution

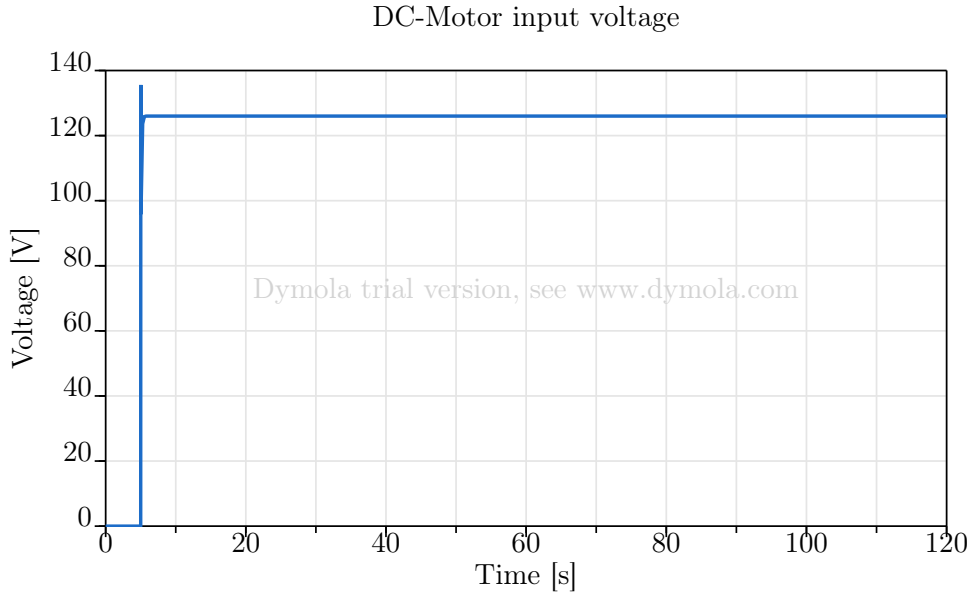

Figure 15: DC-Motor input voltage evolution

As for the temperature analysis, Figures 16 and 17 show the gear box's incoming heat flow and temperature respectively. In the steady-state condition, the heat flux achieves a constant value of about 2200 W, while the temperature keeps increasing since no cooling system is implemented. Therefore, the implementation of this cooling system is mandatory for the correct and safe operation of the propeller electric engine. Table 8 retrieves the heat flow and temperature values at $t = 120$ s which will be input as initial conditions for the simulation of the next point.

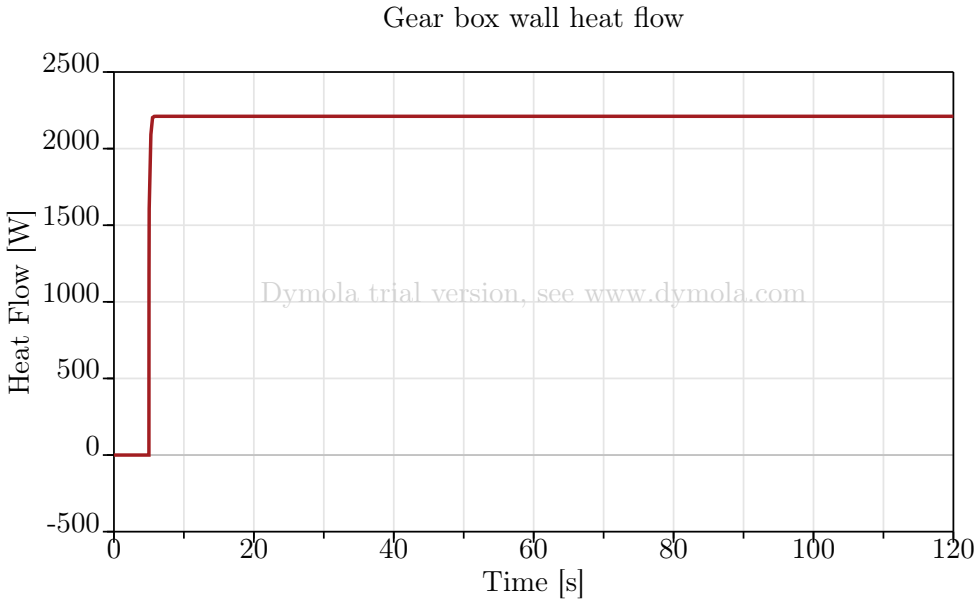

Figure 16: Heat flow in the gear box wall evolution

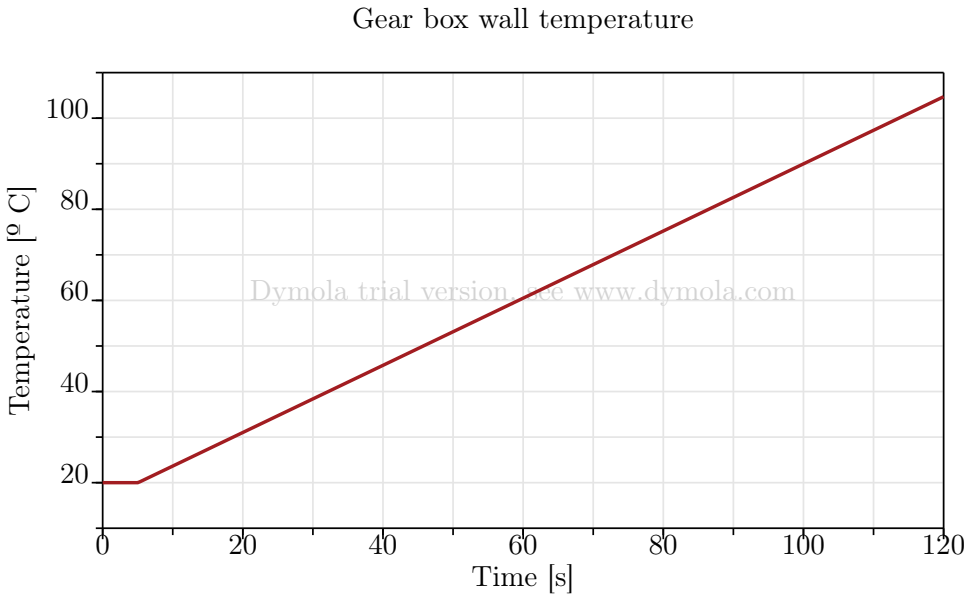

Figure 17: Gear box wall temperature evolution

Heat Flow [W]	**Temperature** [°C]
2210.9	104.7

Table 8: Steady-state gear box wall heat flow and temperatureevolution

2.2) Part 2: Cooling System

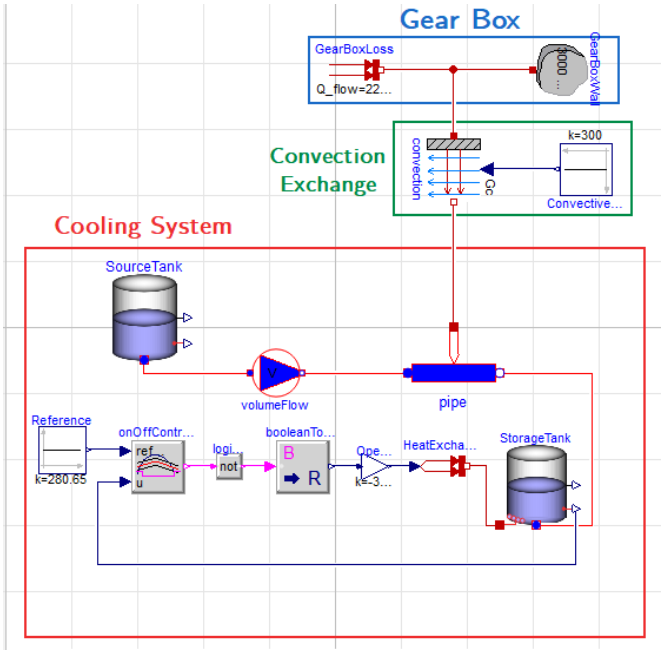

Figure 18: Cooling system physical model

The physical model shown in Figure 18 is retrieved by applying the following assumptions and simplifications:

1. The gear box wall is modelled as a fixed heat flow and a heat capacitor. The conduction block is not included as it has been already considered in the previous simulation
2. The source and storage tanks have the same dimensions as the total water inside the cooling system does not change
3. The cooling system works with a nominal pressure of 1 bar
4. The source tank is initially full of water at 10 °C
5. Water is always flowing from the source tank toward the storage tank with constant volume flow
6. The pipe does have water flowing at $t = 0$ s as the system should be already working due to the gear box wall's initial temperature. The amount of water mass inside the pipe can be retrieved using the water's density and the pipe's dimensions
7. The interaction between the pipe and the gear box wall is modelled as a simple convection heat exchange
8. To cool down the sink-heated water, a heat exchanger is implemented. It is assumed to work always at constant power and is controlled with an on-off logic as it is the typical way in which these kinds of systems work

Before running the simulation, it is necessary to understand the pressure drop inside the pipe due to friction losses. To do so, the Hazen-Williams equation, introduced in Equation 7 is used. This is a simple way to estimate pressure drops inside pipes when the flowing fluid is water, where, h_{pipe} is the pipe head loss, L_{pipe} the pipe length, D_{pipe} the pipe diameter,

$Q_{pipe} = 2 \cdot 10^{-5}$ m^3/s the water volume flow in the pipe, $C_{pipe} = 145$ the Hazen-Williams roughness coefficient and $\gamma_{H2O} = 9804$ N/m^3 the water specific weight.

$$\begin{cases} h_{pipe} = \dfrac{10.593\, L_{pipe}\, Q_{pipe}^{1.85}}{C_{pipe}^{1.85}\, D_{pipe}^{4.87}} \text{ [m]} \\ dp_{pipe} = \gamma_{H2O}\, h_{pipe} = 0.054 \text{ [Pa]} \end{cases} \tag{7}$$

As for the solver, the same discussion as in the previous point applies. Since the model includes domains with different time responses, it probably represents a stiff system which needs to be solved by an A-stable or implicit method. Therefore, the same *DASSL* integration scheme is used. The water volume flow is set to a constant value of $\mathbf{Q_{pipe} = 2 \cdot 10^{-5}}$ m^3/s.

Figure 19 represents the temperature evolution of the gear box wall. It is clear that the cooling system properly works since, after 20 seconds, the temperature enters the admissible threshold specified in the exercise statement and it reaches a steady-state condition also inside the admissible band. Moreover, Figure 20 displays the source tank level during the simulation, which does not get empty during the simulation time, meeting the requirement imposed.

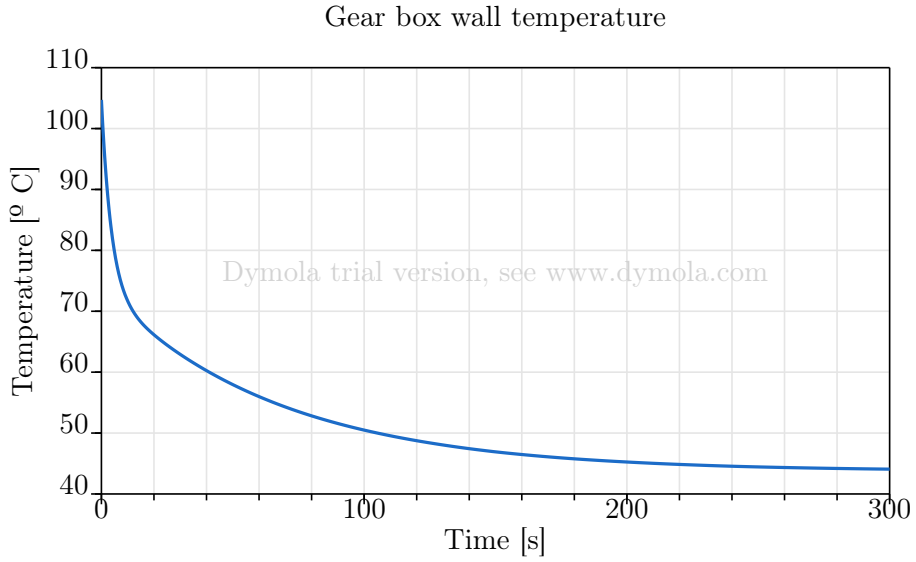

Figure 19: Gear box wall temperature evolution

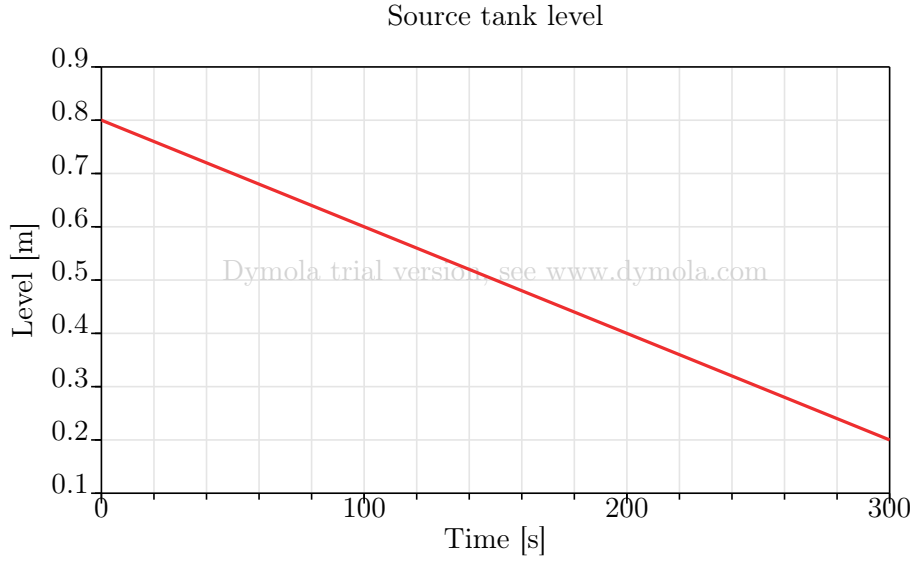

Figure 20: Source tank level evolution

Finally, Figures 21 and 22 display the temperature of the water at the storage tank and the heat exchanger operation during the simulation respectively. The temperature is always in between the specified band, and the heat exchanger's constant power consumption is set to 3750 W as lower values were not capable of cooling down the heated water during the whole simulation time. The power exchanged between the sink-heated water and the heat exchanger is always negative as the last one is removing heat from the stored fluid.

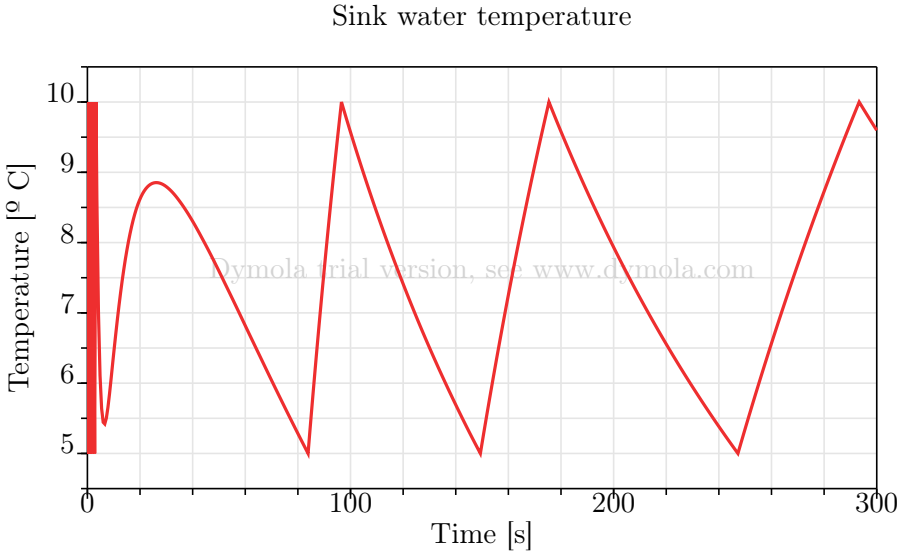

Figure 21: Sink water temperature evolution

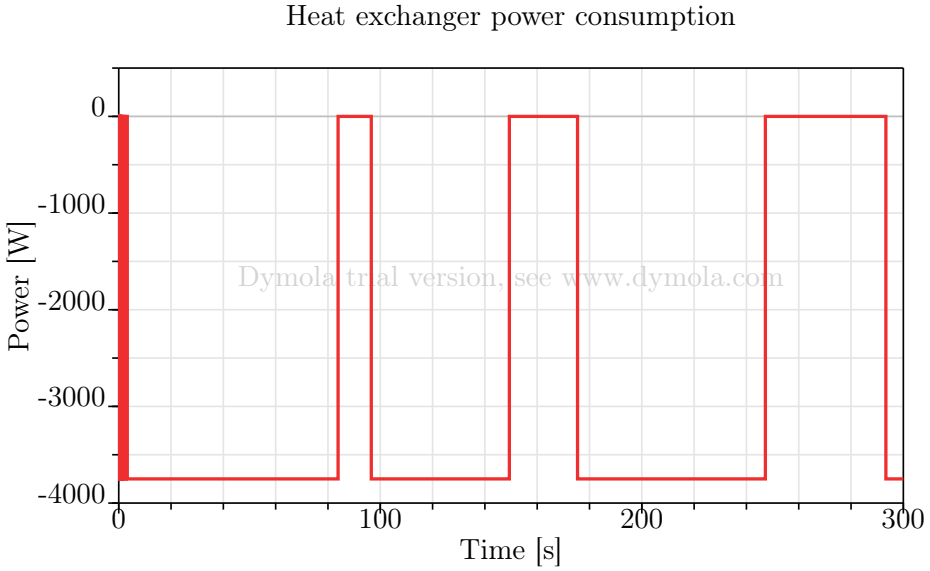

Figure 22: Heat exchanger power consumption evolution

Therefore, the cooling system has been successfully implemented. It keeps the gear box wall temperature in the requested threshold and it always keeps the stored water in the specified temperature range to use it in the following cooling processes.